First-principles calculations of boron-rich compounds of $B_{13}N_2$ and $B_{12}C_2X$ (X = Si, Ge)

2008 J. Phys.: Condens. Matter 20 505211

(http://iopscience.iop.org/0953-8984/20/50/505211)

J. Phys.: Condens. Matter **20** (2008) 505211 (6pp) doi:10.1088/0953-8984/20/50/505211

First-principles calculations of boron-rich compounds of $B_{13}N_2$ and $B_{12}C_2X$ (X = Si, Ge)

Huiyang Gou, Jingwu Zhang and Faming Gao

Department of Applied Chemistry, College of Material Science and Engineering, Yanshan University, Qinhuangdao 066004, People's Republic of China

E-mail: fmgao@ysu.edu.cn

Received 9 May 2008, in final form 2 October 2008
Published 12 November 2008
Online at stacks.iop.org/JPhysCM/20/505211

Abstract

Recently, Kurakevych *et al* (2007 *Acta Crystallogr.* C **63** 80) synthesized the boron-rich phase $B_{13}N_2$ by a high-temperature and high-pressure technique. Here, we performed the non-spin-polarized and spin-polarized calculations for $B_{13}N_2$ by mean of first-principles calculations based on density functional theory. Our calculations show that the magnetic states are more energetically stable than the nonmagnetic state. The elastic and electronic structure calculations demonstrate that the compound of $B_{13}N_2$ is a stable magnetic half-metallic solid. The magnetic properties of $B_{13}N_2$ mainly come from the partially filled *p* states of the boron atom and the considerable interstitial regions. The calculated hardness of $B_{13}N_2$ is 40.8 GPa, indicating a potentially superhard material. Moreover, the similar boron-rich phase $B_{12}C_2Ge$ is predicted to be of the highest hardness among all of the boron-rich phases.

(Some figures in this article are in colour only in the electronic version)

B_{12}-based boron-rich compounds have attracted significant attention due to their fascinating properties, such as great hardness, low density, high strength and thermal stability, and potential technical applications [1–5]. Considerable experimental efforts have been devoted to determining the structure and physical properties of B_{12}-based boron-rich compounds, such as $B_{13}C_2$, $B_{12}O_2$, $B_{12}P_2$, and $B_{12}As_2$ [6–12]. These results indicate that the compounds $B_{13}C_2$ and $B_{12}O_2$ are superhard materials [8–12]. At the same time, the structural, elastic, electronic, optical, vibrational and mechanical properties of $B_{13}C_2$, $B_{12}O_2$, $B_{12}N_2$, $B_{12}P_2$, and $B_{12}As_2$ have been calculated theoretically to understand and even predict the physical and chemical nature of these boron-rich compounds [13–20]. Most recently, a novel boron-rich compound, $B_{13}N_2$, has been synthesized under extreme conditions. The compound of $B_{13}N_2$ crystallizes in the rhombohedral $R\bar{3}m$ (No. 166) structure as determined by the x-ray powder diffraction [21]. However, the detailed physical properties of the rhombohedral $B_{13}N_2$ are not that well explored due to the difficulty in obtaining adequately sized single crystals. First-principles calculation is a well-known and powerful tool to predict the properties and bonding of a material and is thus highly desirable to perform. So far no first-principles calculations on the $B_{13}N_2$ crystal have been reported. Furthermore, among the B_{12}-based boron-rich solids, B_{12} icosahedra links together by X–X chains or X–Y–X chains (X = C, N, O, P, and As; Y = B, Be, Zn, Cd, *et al*) [13–20, 22]. The larger interstitial distance in the chains can possibly accept other elements to form novel compounds. These extraordinary properties render the B_{12}-based boron-rich solids a class of special materials [22–25]. In this paper, we performed first-principles calculations for $B_{13}N_2$; both non-spin-polarized and spin-polarized calculations are considered. Our results show that the magnetic state is preferred over the nonmagnetic state. Furthermore, the elastic and electronic properties of $B_{13}N_2$ are also analyzed. The calculations demonstrate that the compound of $B_{13}N_2$ is a stable magnetic half-metallic solid. In addition, the calculated hardness of $B_{13}N_2$ is 40.8 GPa, indicating a potentially superhard material. Moreover, novel superhard boron-rich phases $B_{12}C_2X$ (X = Si, Ge) are also predicted.

Our first-principles calculations are performed with the CASTEP code [26] based on density functional theory (DFT). The exchange and correlation functional was treated by both

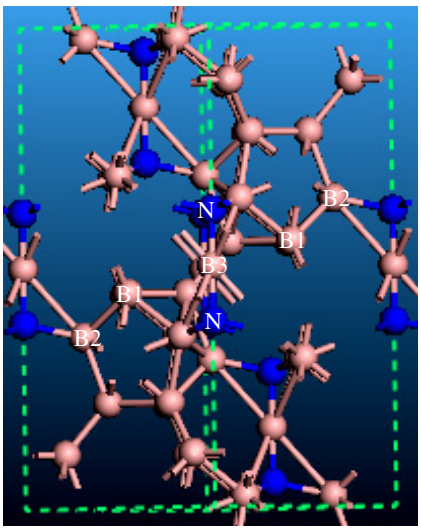

Figure 1. Crystal structure of icosahedral $B_{13}N_2$.

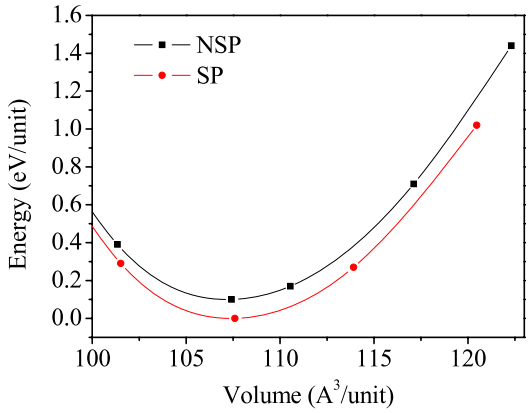

Figure 2. The volume dependence of the total energy calculations, both spin-polarized (SP) and non-spin-polarized (NSP), for $B_{13}N_2$.

the generalized gradient approximation (GGA), as proposed by the Perdew–Burke–Ernzerhof (PBE) [27], and the local density approximation (LDA) used the Ceperley–Alder expression as parametrized by Perdew and Zunger (CAPZ) [28]. The Vanderbilt ultrasoft pseudo-potential [29] was used with a cutoff energy of 500 eV and the k-points of $12 \times 12 \times 12$ are generated using the Monkhorst–Pack scheme for the presently studied $B_{13}N_2$ [30]. For comparison, we also calculated $B_{13}C_2$ with the same structure. The convergence tolerances for geometry optimization were set as a maximum energy change within 5×10^{-6} eV/atom, a maximum ionic Hellmann–Feynman force within 0.01 eV Å^{-1}, a maximum ionic displacement within 5×10^{-4} Å, and a maximum stress within 0.02 GPa. Mulliken overlap populations [31] were integrated with a distance cutoff of 3 Å.

The studied compound $B_{13}N_2$ with the rhombohedral $R\bar{3}m$ (No. 166) structure is built up of B_{12} icosahedra linked together by N–B–N chains [21]. Figure 1 shows the rhombohedral crystal structure of $B_{13}N_2$. In this structure, the polar boron (B1) and equatorial boron (B2) atoms form a B_{12} icosahedron, another boron (B3) atom joins the two nitrogen (N) atoms forming the N–B–N chains and each of the two N atoms links to three B_{12} icosahedra [6–20]. Moreover, from the analysis of [20] within Pauling's bond valence principle, we know that the B3 atom in the rhombohedral $B_{13}N_2$ structure has one extra valence electron; the charge imbalance occurs in the N–B–N chains. A spin-polarized magnetic moment of 1.0 μ_B may exist in $B_{13}N_2$ according to Hund's rule. Therefore, both spin-polarized (SP) and non-spin-polarized (NSP) are performed for $B_{13}N_2$ and $B_{13}C_2$ in the present calculations. It should be pointed out that in this paper the GGA exchange and correlation functional is performed for the magnetic calculations of boron-rich compounds because LDA calculations are usually not very reliable for magnetic systems [32]. The present calculations show that $B_{13}C_2$ favors a nonmagnetic state, but for $B_{13}N_2$, the calculated magnetic moment is 1.0 μ_B per unit. Moreover, the volume dependence of the total energy calculations of SP and NSP for $B_{13}N_2$ is firstly calculated and displayed in figures 2. The magnetic state is preferred over the nonmagnetic one, and the energy difference between the SP and NSP calculations is 0.1 eV/unit. Nevertheless, both the SP and NSP calculations for $B_{13}N_2$ are given for the sake of completeness. The calculated lattice constants for $B_{13}N_2$ and $B_{13}C_2$, within both LDA and GGA, are shown in table 1. It can be seen that the predicted lattice constants in GGA are larger than those in LDA. The calculated lattice parameters and volume for $B_{13}C_2$ with GGA are in excellent agreement with the experimental data, differing only by 1.2%, 0.8%, and 0.5%, respectively [5]. For $B_{13}N_2$, the calculated lattice constant and volume with GGA-SP is overestimated by 0.6%, 1.2%, and 2.5%, respectively, compared with those of the experimental results [21]. These results indicate the present calculations are reasonable. Moreover, the calculated complete set of zero-pressure elastic constants is also shown in table 1. For the rhombohedral hexagonal structure, its five independent elastic stiffness constants C_{11}, C_{33}, C_{44}, C_{12} and C_{13} are listed in table 1. The elastic stability is checked by the whole set of elastic stiffness constants; c_{ij} satisfies all the below conditions using Born–Huang criterion [33, 34]:

$$c_{12} > 0, c_{33} > 0, c_{66} = (c_{11} - c_{12})/2 > 0,$$
$$(c_{11} + c_{12}) - \frac{2c_{13}^2}{c_{33}} > 0, c_{44} > 0.$$

The rhombohedral $B_{13}N_2$ and $B_{13}C_2$ were found to be stable under ambient conditions. In addition, the polycrystalline bulk modulus (B) and shear modulus (G), as calculated using the single crystal elastic constants of $B_{13}N_2$ and $B_{13}C_2$, according to the Voigt–Reuss–Hill averaging scheme [35], are also shown in table 1. Our results demonstrate that within both LDA and GGA the value of the bulk modulus for $B_{13}C_2$ falls in the range 217–263 GPa [15, 16], while the calculated bulk modulus of $B_{13}N_2$, 242 GPa, is slightly larger than that of $B_{13}C_2$, 220 GPa. Nevertheless, the shear modulus of $B_{13}N_2$ is almost the same as that of $B_{13}C_2$, which may imply similar mechanical properties.

The spin-polarized band structure of $B_{13}N_2$ resulting from GGA is presented in figures 3(a) and (b). The spin degeneracy is split and band structure of $B_{13}N_2$ becomes asymmetric for up and down spins. The spin-up channels cross at the Fermi

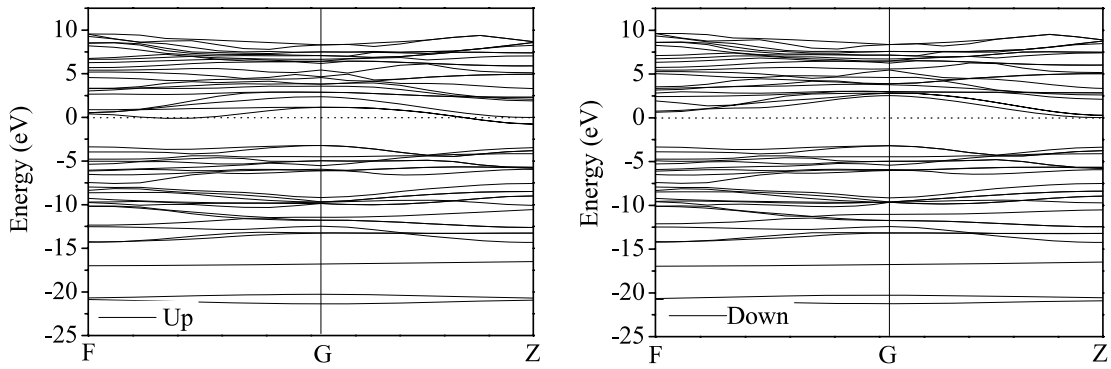

Figure 3. Band structure of half-metallic $B_{13}N_2$: spin-up (left); spin-down (right).

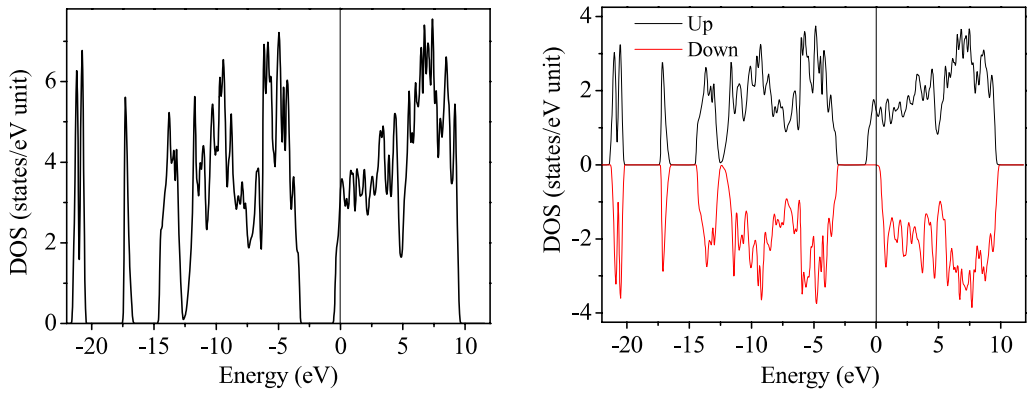

Figure 4. Total density of states (DOS) of non-spin-polarized (left) and spin-polarized (right) $B_{13}N_2$.

Table 1. Calculated lattice parameters, a_0 (Å), c_0 (Å), volume (Å^3), bulk modulus B (GPa), shear modulus G (GPa) compared with available experimental data.

		a_0	c_0	V_0	C_{11}	C_{33}	C_{44}	C_{12}	C_{13}	B	G
$B_{13}N_2$	Expt.[a]	5.4455	12.2649	314.97							
	SP-GGA	5.4788	12.4164	322.778	531	541	108	130	80	242	162
	NSP-GGA	5.4801	12.3907	322.252	517	518	98	131	89	241	151
	NSP-LDA	5.4088	12.2310	309.881	550	539	106	148	96	259	160
$B_{13}C_2$	Expt.[b]	5.6114	12.1908	332.437							
	NSP-GGA	5.6780	12.0927	334.074	517	453	115	118	67	220	162
	NSP-LDA	5.5800	11.9222	321.483	538	471	109	134	74	233	160
	References [15, 16]	5.6168	12.1373	331.607						217–263	
$B_{12}C_2Si$	NSP–LDA	5.5661	12.4677	334.516	522	475	123	134	67	227	166
$B_{12}C_2Ge$	NSP-LDA	5.5776	12.6099	339.732	526	465	132	123	68	228	173

[a] Reference [18]; [b] reference [5].

level exhibiting a metallic character, while the spin-down channels are semiconducting with a much smaller indirect gap of $E_g = 0.04$ eV. The calculated total spin magnetic moment of $B_{13}N_2$ is 1.00 μ_B per formula unit. An integer value of the magnetic moment is a characteristic feature of a half-metallic ferromagnet [36]. At the same time, we also studied the influence of cell volume on the half-metallic ferromagnet because the volume probably affects the dispersion of the band structure. When compressing the volume down to 90% (30 GPa) of equilibrium, the magnetic moment of $B_{13}N_2$ is still stable and retains its integer value. Furthermore, the non-spin-polarized and spin-polarized total density of states (DOS) of $B_{13}N_2$ within GGA is shown in figures 4(a) and (b). From this we notice that the $N(E_F)$ value (3.33 state/eV unit) of the nonmagnetic state at the Fermi level is much larger than that of the magnetic state (1.47 state/eV unit). Such a high DOS at the Fermi energy is sufficient to result in the instability of the nonmagnetic state. According to the Stoner theory of band ferromagnetism [37–40], the large $N(E_F)$ at the Fermi level may suggest the instability of the nonmagnetic state with respect to the onset of intra-band spin polarization. The application of the Stoner criterion here is justified because the nonmagnetic state of the rhombohedral $B_{13}N_2$ is metallic. Furthermore, from figure 4(b), the spin-up band is partially filled while the spin-down band is empty, displaying a 100% spin polarization $P(E) = (N_\uparrow(E_F) - N_\downarrow(E_F))/(N_\uparrow(E_F) +$

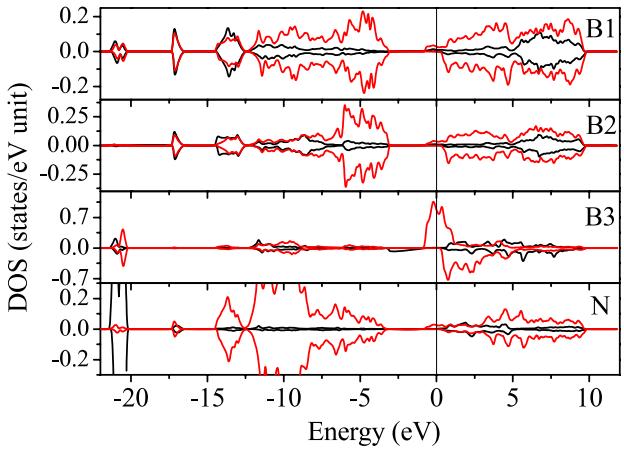

Figure 5. Partial (red curve, p-states and black curve, s-states) density of states of spin-polarized $B_{13}N_2$.

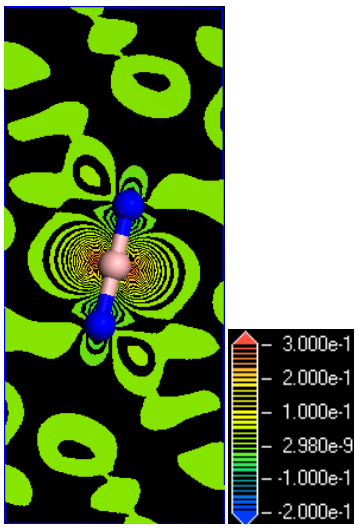

Figure 6. The contour plot of the spin density of $B_{13}N_2$ in the (111) plane. A strongly localized spin polarization is exhibited near the B3 atoms in the N–B–N chain.

$N_\downarrow(E_F)$), where $N(E_F)$ is the density of states of up $\uparrow$ or down $\downarrow$ electrons at the Fermi level [41]. For a better insight into bonding and magnetism, we also show the spin dependent partial density of state (DOS) of $B_{13}N_2$ in figure 5. It can be seen that both the spin-up and spin-down bands in the range energy of -15 and -3 eV show strong N 2p and B 2p hybridization. In the vicinity of the Fermi level the spin-up band is dominated by the 2p states of the B3 atom while the 2p states of the other B atoms and the N 2p states have a relatively smaller contribution. Thus, the major contribution to the magnetic moment of $B_{13}N_2$ may come from the partially filled 2p states of the B3 atom. Nevertheless, the stronger hybridization between N 2p and B 2p evidently decreases the value of magnetic moment in the B3 atom from 1 μ_B (Hund's rule value) to 0.42 μ_B. The contour plot of the spin density is shown in figure 6. From that we can notice that the spin polarization is strongly localized near the B3 atoms and the interstitial regions also have a larger contribution to the magnetic moment.

The aforementioned studied $B_{13}N_2$ crystal has a similar bulk and shear modulus to that of $B_{13}C_2$, and also a strong hybridization in bonding. Also, the well-known boron-rich compounds, such as $B_{13}C_2$, $B_{12}O_2$, are superhard materials [8–20]. It is thus expected that the rhombohedral $B_{13}N_2$ compound is similar. Based on Mulliken overlap population analysis in a first-principles approach [42], we calculate the intrinsic hardness of rhombohedral $B_{13}N_2$ as follows: H_v^μ (GPa) $= 740P^\mu(v_b^\mu)^{-5/3}$, where P^μ is Mulliken overlap population of the μ-type bond, v_b^μ is the volume of bond of type μ. The calculated hardness of $B_{13}N_2$ was listed in table 2. The calculated hardness of the half-metallic $B_{13}N_2$ is 40.8 GPa. This result indicates that the rhombohedral $B_{13}N_2$ crystal is also a potential superhard material. When the interstitial boron site is replaced with the given atom, the hardness of the boron-rich compound may be further increased, such as $B_{12}N_2Be$. Gao *et al* [19, 20] have already designed a series of boron-rich compounds whose structure is the same as that of $B_{13}N_2$. It is the relatively large interstitial doping sites that make the design and synthesis of novel boron-rich compounds to be a possibility [24]. Following this idea, we

Table 2. Calculated Mulliken bond overlap population, P^μ, the volume of the weakest bond of type μ, v_b^μ(3), and the calculated and experimental Vickers hardness of $B_{13}N_2$, $B_{12}C_2Si$ and $B_{12}C_2Ge$, respectively.

Phases	Bond	P^μ	v_b^μ	H_{vcal}	H_{vexpt}
$B_{13}N_2$	B–B	0.42	3.382	40.8	
$B_{12}C_2Si$	B–B	0.46	2.853	59.3	63.7 ± 2.8 [a]
$B_{12}C_2Ge$	B–B	0.50	2.842	64.9	
$B_{12}N_2Be$ [b]	B–B	0.44	2.716	61.6	
$B_{12}O_2$ [b]	B–B	0.38	3.056	43.7	45

[a] Experimental hardness of doped-Si boron-rich phase in [24].
[b] From [42].

design boron-rich compounds $B_{12}C_2X$ (X = Si, Ge) with the structure of the rhombohedral $B_{13}N_2$ crystal in the following section.

The optimized equilibrium structural parameters, single crystal elastic modulus, and bulk and shear moduli of $B_{12}C_2X$ (X = Si, Ge) phases are also given in table 1. The volumes of $B_{12}C_2X$ (X = Si, Ge), due to the replacement of Si or Ge, are only slightly larger than those of $B_{13}C_2$. Nevertheless, the calculated bulk moduli of the $B_{12}C_2X$ (X = Si, Ge) phases are close to that of $B_{13}C_2$, while the shear modulus is slightly increased from $B_{13}C_2$, 160 GPa, to $B_{12}C_2Si$, 166 GPa, to $B_{12}C_2Ge$, 173 GPa. This trend of shear modulus in these boron-rich compounds may imply an increasing hardness from $B_{13}C_2$ to $B_{12}C_2Si$ and to $B_{12}C_2Ge$. We thus calculated the theoretical hardness of the $B_{12}C_2X$ (X = Si, Ge) phases using the intrinsic hardness model [42]; these are also listed in table 2. The calculated results show that the new boron-rich $B_{12}C_2X$ (X = Si, Ge) phases have excellent mechanical properties. The hardness of the $B_{12}C_2Si$ phase, 59.3 GPa, is slightly smaller than that of the experimental estimated hardness of the doped-Si boron-rich phase, 63.7 ± 2.8 GPa [24], but larger than that of $B_{13}C_2$, 58.6 GPa [32]. Moreover, the hardness of the $B_{12}C_2Ge$ phase, 64.9 GPa, surpassing

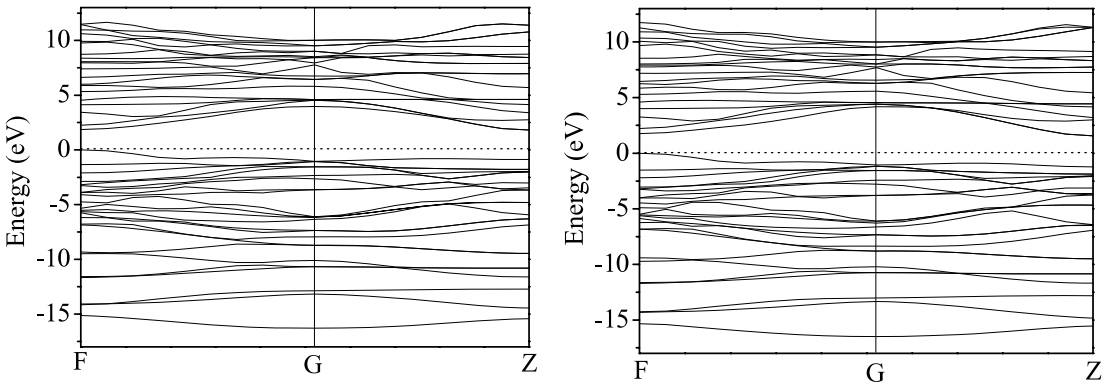

Figure 7. Calculated band structure of $B_{12}C_2Si$ (left) and $B_{12}C_2Ge$ (right) phases.

the other available boron-rich compounds, is only less than that of diamond and cubic boron nitride. Due to the novel mechanical properties, we also calculated the electronic band structure of the $B_{12}C_2X$ (X = Si, Ge) phases displayed in figure 7. It shows that the calculated band structures indicate that both $B_{12}C_2Si$ and $B_{12}C_2Ge$ phases are semiconductor materials. For the $B_{12}C_2X$ (X = Si, Ge) phases, all the conduction band minima occur at the Z point, whereas the valence band maxima are located at the F point making them indirect band gap of 1.81 eV and 1.57 eV, respectively. The band gap of both $B_{12}C_2X$ (X = Si, Ge) phases is smaller than that of $B_{13}C_2$, 3.01 eV [13]. The true band gap of the $B_{12}C_2X$ (X = Si, Ge) phases should be larger by 50%–80% when considered the underestimation of the density functional theory [43]. Therefore, the $B_{12}C_2X$ (X = Si, Ge) phases should possess potential technological applications, once synthesized in experiments, due to their novel mechanical and electronic properties.

In conclusion, we have performed non-spin-polarized and spin-polarized calculations for $B_{13}N_2$ by means of first-principles calculations based on density functional theory. The calculated lattice parameters of $B_{13}N_2$ are in agreement with the available theoretical and experimental values. The calculated total energy indicates that the magnetic half-metallic state is preferred over the nonmagnetic one. Analysis of the electronic structure and spin density shows that the magnetic properties of arise from the partially filled p states of boron atom and the considerable interstitial regions. The intrinsic hardness of $B_{13}N_2$ is also calculated to be 40.8 GPa based on Mulliken overlap population analysis through a first-principles approach, indicating a potentially superhard material. In addition, the novel boron-rich phases $B_{12}C_2X$ (X = Si, Ge) have been designed, the results indicating that they are semiconducting materials with the calculated band gaps of 1.81 eV and 1.57 eV, respectively. The calculated hardness of $B_{12}C_2Si$ and $B_{12}C_2Ge$ are 59.3 and 64.9 GPa, respectively.

Acknowledgments

The authors acknowledge financial support from National Natural Science Foundation of China (Grant 50672080), the Foundation for the Author of National Excellent Doctoral Dissertation of the People's Republic of China (No. 200434), the Science Foundation of Yanshan University for Excellent PhD Students and a Foundation of Hebeirenshiting.

References

[1] Chen M, McCauley J W and Hemker K J 2003 *Science* **299** 1563
[2] Mauri F, Vast N and Pickard C J 2001 *Phys. Rev. Lett.* **87** 085506
[3] Domnich V, Gogotsi Y, Trenary M and Tanaka T 2002 *Appl. Phys. Lett.* **81** 3783
[4] Emin D 1987 *Phys. Today* **40** 55
[5] Emin D, Aselage T L, Switendick A C, Morosin B and Eckel C L 1990 *Boron-Rich Solids* (New York: AIP)
[6] Kirfel A, Gupta A and Will G 1979 *Acta Crystallogr.* B **35** 1052
[7] Armstrong D R, Bolland J, Perkins P G, Will G and Kirfel A 1983 *Acta Crystallogr.* B **39** 324
[8] Rizzo H F, Simmons W C and Bielstein H O 1962 *J. Electrochem. Soc.* **109** 1079
[9] Lundstron T and Andreev Y G 1996 *Mater. Sci. Eng.* A **209** 16
[10] Lundstron T 1997 *J. Solid State Chem.* **133** 88
[11] Hubert H, Devouard B, Garvie L A J, Keeffe M O, Buseck P R, Petuskey W T and McMillan P F 1998 *Nature* **391** 376
[12] He D, Zhao Y, Daemen L, Qian J, Shen T D and Zerda T W 2002 *Appl. Phys. Lett.* **81** 643
[13] Bylander D M and Kleinman L 1991 *Phys. Rev.* B **43** 1487
[14] Lee S, Kim S W, Bylander D M and Kleinman L 1991 *Phys. Rev.* B **44** 3550
[15] Lee S, Bylander D M and Kleinman L 1992 *Phys. Rev.* B **45** 3245
[16] Li D and Ching W Y 1995 *Phys. Rev.* B **52** 17073
[17] Li D and Ching W Y 1996 *Phys. Rev.* B **54** 1451
[18] Morrison I, Bylander D M and Kleinman L 1991 *Phys. Rev.* B **45** 1533
[19] Gao F M, Hou L and He Y H 2004 *J. Phys. Chem.* B **108** 13069
[20] Gao F M, Qin X J, Wang L Q, He Y H, Sun G F, Hou L and Wang W Y 2005 *J. Phys. Chem.* B **109** 14892
[21] Kurakevych O O and Solozhenko V L 2007 *Acta Crystallogr.* C **63** 80
[22] Gou H Y, Hou L, Zhang J W, Sun G F, Gao L H and Gao F M 2008 *Phys. Status Solidi* b **245** 58
[23] Emin D 2004 *J. Solid State Chem.* **177** 1619
[24] Niemyski T, Appenheimer S, Panczyk J and Badzian A 1969 *J. Cryst. Growth* **5** 401
[25] Hyodo H, Araake S, Hosoi S, Soga K, Sato Y, Terauchi M and Kimura K 2008 *Phys. Rev.* B **77** 024515

[26] Clark S J, Segall M D, Pickard C J, Hasnip P J, Probert M J, Refson K and Payne M C 2005 *Z. Krystallogr.* **220** 567
[27] Perdew J P, Burke K and Ernzerhof M 1996 *Phys. Rev. Lett.* **77** 3865
[28] Ceperley D M and Alder B J 1980 *Phys. Rev. Lett.* **45** 566 Perdew J P and Zunger A 1981 *Phys. Rev.* B **23** 5048
[29] Vanderbilt D 1990 *Phys. Rev.* B **41** 7892
[30] Monkhorst H J and Pack J D 1976 *Phys. Rev.* B **13** 5188
[31] Mulliken R S 1955 *J. Chem. Phys.* **23** 1833
[32] Wu Z J and Meng J 2007 *Appl. Phys. Lett.* **90** 241901
[33] Born M 1940 *Proc. Camb. Phil. Soc.* **36** 160
[34] Born M and Huang K 1956 *Dynamical Theory of Crystal Lattices* (Oxford: Clarendon)
[35] Hill R 1952 *Proc. Phys. Soc. Lond.* **65** 350
[36] Gao G Y, Yao K L, Şaşıoğlu E, Sandratskii L M, Liu Z L and Jiang J L 2007 *Phys. Rev.* B **75** 174442
[37] Janak J F 1977 *Phys. Rev.* B **16** 255
[38] Sieberer M, Khmelevskyi S and Mohn P 2006 *Phys. Rev.* B **74** 014416
[39] Houari A, Matar S F, Belkhir M A and Nakhl M 2007 *Phys. Rev.* B **75** 064420
[40] Matar S F, Houari A and Belkhir M A 2007 *Phys. Rev.* B **75** 245109
[41] Durgun E, Cakir D, Akman N and Ciraci S 2007 *Phys. Rev. Lett.* **99** 256806
[42] Gao F M 2006 *Phys. Rev.* B **73** 132104
[43] Kroll P 2003 *Phys. Rev. Lett.* **90** 125501